scientific reports

Check for updates

OPEN

Applications of Opuntia ficus-indica (L.) mill seed oil from eastern morocco including chemical profiling, antibacterial activity, and docking

Salma Kadda[1]✉, Oussama Khibech[2], El Hassania Loukili[1], Raffaele Conte[3], Khalil Azzaoui[4], Sabir Ouahhoud[5], Belkheir Hammouti[1], Hana Caid Serghini[6], Taibi Ben Hadda[1], Shehdeh Jodeh[7]✉ & Abdelmajid Belabed[6]

This study reports the chemical profiling and antimicrobial potential of *Opuntia ficus-indica* seed oil from Eastern Morocco, with emphasis on pharmacologically relevant constituents and valorization of an underexploited by-product. Seed oil was obtained by cold mechanical pressing and characterized using GC–MS (fatty acids and volatile profile), HPLC–DAD (tocopherols), and UHPLC–MS/MS (phenolic constituents). The oil exhibited a PUFA-rich profile dominated by linoleic acid (73.94%), with palmitic and stearic acids as major saturated components, while oleic acid was not detected under our analytical conditions. Tocopherol analysis revealed a high γ-tocopherol level (657.52 mg/kg). UHPLC–MS/MS enabled annotation of multiple phenolic compounds, including arbutin and kaempferol as major constituents. In vitro antibacterial assays showed no inhibition against *Staphylococcus aureus* and *Streptococcus* spp. (inhibition zone < 7 mm), whereas moderate-to-high activity was observed against *Escherichia coli* (11.6 ± 0.64 mm) and *Klebsiella* spp. (15.6 ± 0.51 mm). In silico POM analysis supported favorable drug-likeness/toxicological profiles for arbutin and kaempferol. Overall, these results support *O. ficus-indica* seed oil as a chemically rich natural matrix with promising antioxidant and antibacterial potential.

Keywords Opuntia ficus-indica, Linoleic acid, Tocopherols, Phenolic profile, Antibacterial activity, POM analysis, good health and wellbeing

Aromatic and medicinal plants have long inspired researchers because their volatile and lipidic fractions provide chemically diverse natural matrices with applications spanning biology, therapeutics, organic chemistry, food technology, perfumery, and cosmetology. Beyond essential oils, vegetable seed oils are increasingly valued as multifunctional materials: they are major dietary energy sources and, importantly, they deliver essential fatty acids, phytosterols, tocopherols (vitamin E), pigments, and phenolic components that can jointly influence oxidative stability and biological activity[1]. In parallel, the growing demand for natural antimicrobial and antioxidant agents is accelerating interest in seed oils rich in bioactive lipids and phenolics, especially when they originate from agro-industrial by-products that can be sustainably valorized[2]. In this context, *Opuntia ficus-indica* (prickly pear cactus) has emerged as a high-potential resource, not only through its edible pulp but also through its seed fraction, which is often discarded despite its bioproduct value. Several studies report that cactus seeds exhibit a low to moderate oil yield (commonly in the from 5 to 15% range depending on

[1]Euromed University of Fes (UEMF), Fez 30000, Morocco. [2]Faculty of sciences, department of Chemistry, Laboratory of Applied and Environmental Chemistry (LCAE), Mohammed Premier University, University Mohammed Premier, Oujda, Morocco. [3]Research Institute on Terrestrial Ecosystems (IRET)—CNR, Via Pietro Castellino 111, Naples 80131, Italy. [4]Engineering Laboratory of Organometallic, Molecular Materials and Environment, Faculty of Sciences, Sidi Mohamed Ben Abdellah University, Fes 30000, Morocco. [5]Faculty of Medicine and Pharmacy, Sultan Slimane University, Beni Mellal, Morocco. [6]Laboratory of Plants & Microorganisms Biology, Faculty of Sciences, Oujda – University Mohammed Premier, Oujda BP-717, 60000, Morocco. [7]Department of Chemistry, An-Najah National University, P.O. Box 7, Nablus, Palestine. ✉email: salma.kada25@gmail.com; sjodeh@najah.edu

cultivar, environment, and extraction), making them a realistic target for circular-economy valorization[3]. Chemically, cactus seed oil is typically dominated by linoleic acid[1], the oil is also notable for high levels of tocopherols and phytosterols, with γ-tocopherol and β-sitosterol frequently predominant. Alongside the lipid fraction, profiling of volatile constituents is relevant because the aroma/oxidation-derived volatiles reflect both quality and potential functional attributes; in Morocco, dynamic headspace GC–MS investigations have mapped characteristic volatile markers in cactus seed oil[4]. Building on this background, the objective of the present study is to provide an integrated chemical characterization of *O. ficus-indica* seed oil sourced from Eastern Morocco by combining complementary analytical platforms: HS-GC–MS (volatiles), GC–MS (fatty acids), HPLC–DAD (tocopherols), and UHPLC–MS/MS (phenolic annotation), and to relate these chemical signatures to in vitro antibacterial outcomes[4]. The novelty of our work lies in two main aspects. First, we deliver a single, consolidated multi-platform dataset that captures, in one coherent framework, the major (fatty acids) and minor (volatiles, tocopherols, phenolics) fractions of Eastern Moroccan cactus seed oil an approach that addresses the frequent fragmentation of prior reports[2]. Second, we complement experimental antibacterial testing with a POM-based in silico analysis (PETRA/OSIRIS/Molinspiration) and docking to rationalize the bioactivity potential of two abundant phenolic constituents, arbutin and kaempferol, using a workflow that has been used in the literature to rapidly estimate physico-chemical descriptors, drug-likeness indicators, and toxicity/bioactivity relevant flags[5,6]. Together, this integrated chemistry-function strategy supports the sustainable valorization of *O. ficus-indica* seeds as a high-value by-product with promising applications in food, cosmetic, and pharmaceutical oriented formulations[7].

Materials and methods

Sampling air

O. ficus-indica was collected from a non-protected public area in Guerbouz (Berkane Province, Eastern Morocco) Fig. 1. Sampling was conducted in accordance with local and institutional guidelines, and no protected species were targeted.

Voucher number

The plant was identified and confirmed by Professor Fennane Mohammed a professional botanist, of the Scientific Institute of Rabat, Morocco. The *Opuntia ficus-indica* L. specimen was deposited in the botanical section of the Herbarium of Mohammed first University in Oujda, Morocco (HUMPOM), under reference number (HUMPOM745)[8].

Morphological description

Prickly pear seeds are dicotyledonous seeds enclosed in fruits (Angiosperms). They are hard and 5 millimeters (mm) in diameter[9](Fig. 2). A morphological study of the seed using scanning and transmission electron microscopy reveals the organization of the tissues into two parts: The pericarp: represents up to 90% of the total weight of the seed; it is made up of two types of cells: mostly very compact long cells in the form of spindle fibers (sclerenchyma) who is cellulose microfibrils are arranged in successive concentric layers. And those constituting single-helix spiral conductor vessels[10]. Up to 10% of the seed's weight is made up of the endosperm, which is composed of reserve parenchyma cells with fragile walls and many leucoplasts that form tiny starch grains. The

Fig. 1. Picture of prickly pear seeds.

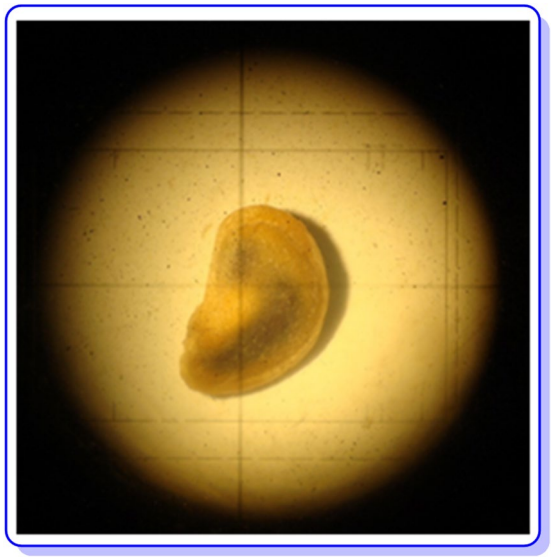

Fig. 2. View of *Opuntia Ficus indica* seed from Eastern region of Morocco under binocular loupe.

Fig. 3. Oil press of *Opuntia Ficus indica* seeds of Eastern Morocco.

gluten layer (also known as the aleurone layer) that lies between the starch-rich tissues gives the nucleus its viscous appearance. A thick, inverted tile-shaped cell wall surrounds each of these cells[10].

Extraction

The extraction method is cold pressing using a mechanical process that requires no chemicals (Fig. 3). It involves passing the seeds through a screw press. Extraction machine made in Morocco Ste les Ateliers Afyach, (Fig. 3) brand P55/AFYACH, voltage 220/380 V, year of manufacture 2019. The oil is then decanted and filtered several times through several filter papers to remove residual seed debris[11] Extractions are obtained using a mechanical press at low temperature The oil yields from OFI seeds are reported in Extract yields (w/w) are calculated as the ratio between the mass of extract obtained and the mass of the dried samplé.

$$Y\ (\%)\ =\ ((M1)\ /M2))\ x\ 100$$

Preparation of extracts

200 milliliters of hexane and 100 milliliters of oil are macerated for 24 h at room temperature with magnetic stirring, while the flasks are shielded from light with aluminum foil. After that, the macerate is gathered and centrifuged. A filter crucible (Porosity 4) was used to filter the supernatant. The maceration process was then repeated using three organic solvents in order to obtain the corresponding extracts: ethanol, water, and ethyl acetate. Before being used, the extracts were stored at 4 °C in dark bottles.

Determination of total polyphenols

The total phenol content of the ethanolic extract (DO) was determined using the Folin-Ciocalteau procedure, with certain modifications. To build the calibration curve 200 µL of ethanolic gallic acid standard solution at various concentration (0.78, 1.56, 3.12, 6.25, 12.5, 25, 50, and 100 µg/mL) wre combined with 1mL of Folin-Ciocalteu reagent and 800 µL (75 g/L) of sodium carbonate (Na_2CO_3). The mixture was allowed to react for during one hour under incubation. Following this, the degree of absorption at a specific wavelength of 765 nm is measured and subsequently compared with the standard value of ethanol. It is imperative that all measurements be performed in triplicate. Total Phenolic content was expressed as mg gallic acid equivalents (GAE) per 100 mg dry weight extracted from the sample[11].

Flavonoid analysis

The quantification of flavonoid content is executed in accordance with the methodology delineated by Kim et al. (2012) [12], with minor adaptations. In a suitable container, combine 200 µL of ethanolic extract were mixed with 1,000 µL of distilled water and 50 µL of $NaNO_2$ (5%). after six-minute interval, 120 µL of $AlCl_3$ (10%) solution was introduced, and the mixture was left five-minute incubation period. Subsequently, 400 µL of NaOH (1 M) and 230 µL of distilled water were added. Standard curve is established using a standard solution of quercetin at different concentrations (0.78, 1.56, 3.12, 6.25, 12.5, 25, 50, and 100 µg/mL). Methanol is utilized as a blank to measure the degree of light absorption at 510 nm. Each assay is repeated thrice consecutively. The total phenol concentration data are expressed in terms of quercetin equivalents (QE) per milligram of extracted sample dry matter[12].

Chromatographic profiles

Gas chromatography GC-MS

Equipment and analysis conditions: Incubation of samples at 50 °C for 15 min. Subsequently, 500 µL of the gas phase produced is injected into the Gas chromatography (split ratio 1:10) using the gas-tight syringe of the AOC-6000 headspace autosampler (PAL system) connected to the GC-MS-QP2020 NX coupled with a mass spectrometer (Shimadzu). GC/MS column: ZB-Semivolatiles capillary column 30 m × 0.25 mm × 0.25 µm thick. Over: 40 °C (2 min) → 10 °C/min → 150 °C → 10 °C/min → 200 °C. Carrier gas: He (helium), Injection temperature: 150 °C, Ionization voltage: 70 eV, Ion source temperature: 200 °C, The mass detector was set to scan mode (event duration, 0.30 s; scan speed, 3333) from 20 to 800 m/z.The analytes are identified by their fragmentation profiles using the NIST17-1 library[13].

Volatile compounds GC-MS analysis

The volatile constituents of oil were characterized by GC–MS using a Shimadzu GC system (Kyoto, Japan) coupled to a QP2010 mass spectrometer and fitted with a BPX25 capillary column (30 m × 0.25 mm i.e., 0.25 µm film; 5% diphenyl/95% dimethylpolysiloxane)[14]. Helium (99.99%) was used as the carrier gas at a constant flow of 1.69 (unit as reported)[14]. The injector, ion source, and interface temperatures were maintained at 250 °C. The oven program started at 50 °C (1 min), increased to 250 °C at 10 °C min^{-1}, and was held for 1 min. Samples (1 µL) were introduced in split mode, and mass spectra were acquired under electron ionization (EI) at 70 eV over an m/z range of 40–300. Compound identification was achieved by matching retention times and EI fragmentation patterns with the NIST mass spectral library, supported by standard GC–MS identification practice for essential oils[15]. Data acquisition and processing were performed using LabSolutions/GC: MSsolution software (v2.5, Shimadzu)[16].

HPLC-DAD chromatography

The tocopherols were analyzed on a Hewlett-Packard liquid chromatograph (HPLC) system (model LC-6AD) with a diode array detector (DAD) that was modified to suit the analysis. Method 14 was modified for this analysis. Subsequent purification was executed through use of a 250 mm silica-NH_2 column (Ultrasphere), possessing an internal diameter of 4.6 mm and a porosity of 5 µm. This column was employed within a mobile phase consisting of a mixture of hexane/isopropanol (99/1 V/V), at a flow rate of 1 ml/min. The identification process was executed through the utilization of α-, β-, γ-, and δ-tocopherol standards (purchased from Sigma-Aldrich, St. Louis, USA), with the analysis conducted at 292, 296, and 298 nanometers. Subsequently, the concentration of tocopherol was computed based on the established external calibration curve [14].

Ultra-high performance liquid chromatography MS/MS (UHPLC–MS/MS)

Approximately 80 mg of ethanolic extract was subjected to sonication for 60 min at 45 °C. The phenolic compound of this analysis was characterized using (Nexera XR LC 40) UHPLC system equipped with an MS/MS detector (LCMS 8060, manufactured by Shimadzu Italy in Milan, Italy). This instrument is utilized to characterize the phenolic profile of the sample under examination. Chromatographic separation was achieved using a Phenomenex Kinetex Polar C18 column (2.6 µm particle size). The injection volume was 10 µL. Mass spectrometric analysis was performed using electrospray ionization (ESI) operated in negative ion mode (ESI−), except for syringic acid, which was analyzed in positive ion mode (ESI+). The nebulizer gas flow was set at 2.9 L/min, the heating gas at 10 L/min; interface temperature at 300 °C Desolvation line temperature is set at 250 °C; and heat block temperature at 400 °C, and the drying gas flow rate was maintained at 10 L/min. The mobile phase was composed of a single solvent: acetonitrile and water with 0.01% formic acid (5:95, v/v). The confirmation of molecular identification was achieved through a comparison of the identified fragment with those stored within the in-house molecule library[11].

Antimicrobial activity

To evaluate antibacterial activity (two gram-positive bacterial strains and four gram-negative strains), we used the agar diffusion test (antibiogram). Widely used in microbiology, this diffusion method relies on the diffusion of an antimicrobial compound through a solid medium. The antimicrobial product's impact on the target is evaluated by measuring the inhibition zone. The microbial strain will be classified as sensitive, intermediate, or resistant based on the diameter of the inhibition zone. Diffusion of the test product and growth of the microorganism compete in the diffusion technique. The standard reference strains used are *S. aureus* (ATCC25923), *Streptococcus spp* (ATCC19615), *E. coli* (ATCC 25922), and *Klebsiella spp* (ATCC13883). All strains were stored at the Laboratory for Agricultural Production Improvement, Biotechnology, and Environment at the Faculty of Sciences of Oujda, Mohammed I University.

Procedure

The antibacterial activity was assessed using the agar well-diffusion test, with modifications. Approximately 15 mL of melted agar maintained at 45 °C was transferred into sterile Petri dishes (Ø 90 mm). Bacterial stains suspensions were freshly prepared and distributed over the Mueller-Hinton agar plates. Once the agar surface had dried under antiseptic conditions, wells of 6-mm were pierced into the agar using a sterile Pasteur pipette. A volume of 100 µL of each OFI oil extract solution (100 mg/mL) was deposited into the designated wells. The plates were subsequently incubated at 37 °C for 24 h. DMSO was utilized as a negative control[17], while gentamicin, an antibiotic, and lactic acid, at equivalent concentrations, were employed as positive controls. Antimicrobial potency was evaluated by measuring the diameter of the circular inhibition zones. The extent of antimicrobial activity is delineated by the inhibition zone, which encompasses the diameter of the disc[18]. The tests were performed in triplicate.

Antifungal activity

PDA (Potato Dextrose Agar) preparation culture medium

We added 39 g of PDA to 1 L of distilled water, agitated and boiled for 10 min, then sterilized the PDA medium at 120 °C for 20 min in autoclave.

Preparation of FOA (Fusarium Oxysporum Albidinis) fungus

Fusarium oxysporum has been identified as the causative agent in cases of "Bayoud," as evidenced by its presence in xylem tissue and the manifestation of characteristic symptoms. The extraction of vascular tissue fragments proceeded under aseptic conditions, wherein the fragments were placed in PDA medium prior to undergoing incubation at 28 °C. *Fusarium oxysporum* identification isolates was based on their morphological characteristics[17]. A monoconidium of *Fusarium oxysporum* was isolated on a PDA medium at a temperature of 28 °C[17].

Sample preparation and Fusarium test

A quantification of 100 mg of oil was dissolved in 1 mL of DMSO (dimethyl sulfoxide) to obtain a stock solution of 100 mg/mL solution. The solution was utilized as a foundation for the subsequent steps. Volumes of 50 µl, 75 µl, and 150 µl were meticulously dispensed into sterile tubes. Thereafter, sterile PDA (potato dextrose agar) liquid was added to obtained a final volume of 10 ml. Place the mixture in 8.5 cm diameter Petri dishes and allow the medium to stand until solidified. Once the agar surface was an FOA pellet had been placed in the center of each plate, which had already grown on the solid PDA. The dishes were incubate for four days at a temperature of 28 °C. the FOA diameter in treated plates compare with a control comprising only DMSO at a specific dose (control) yielded results expressed as a percentage of inhibition[19].

$$Percentage\ inhibition\ =\ (D0 - Dx)/D0\ x\ 100$$

$$D0\ =\ diameter\ in\ cm\ of\ the\ FOA\ in\ the\ control$$

$$Dx\ =\ diameter\ in\ cm\ of\ the\ FOA\ in\ the\ test$$

Molecular docking methodology

Protein structures were retrieved from the RCSB Protein Data Bank and selected to represent bacterial type II topoisomerase targets (DNA gyrase subunit B and topoisomerase IV) relevant to the observed antibacterial activity, together with a fungal sterol 14α-demethylase model (CYP51B) to contextualize the lack of antifungal activity. The docking panel included 3U2D (*Staphylococcus aureus* GyrB ATPase domain), 5MMP (*Escherichia coli* GyrB ATPase domain), 1S16 (*E. coli* ParE ATPase domain), 6WAA (topoisomerase IV ParE–ParC DNA-associated complex), and 6CR2 (fungal CYP51B). The two investigated metabolites, arbutin (10) and kaempferol (42), were prepared in PyRx 0.9, converted to the required format, and energy-minimized prior to docking. Receptor preparation was performed using AutoDockTools 1.5.7 by removing non-essential heteroatoms, adding polar hydrogens, assigning Gasteiger charges, and exporting the structures in PDBQT format; for CYP51B, the prosthetic group required for catalytic-site integrity was retained, and for the topoisomerase IV cleavage complex the structural context of the binding region was preserved. Docking calculations were conducted using AutoDock Vina 1.2.0 with grid boxes centered on the co-crystallized ligand/active-site region of each target to ensure consistent sampling of the functional binding pocket, and binding affinities were reported as Vina scores (kcal/mol)[20,21]. The docking workflow was validated by redocking the native co-crystallized ligands into their corresponding proteins and calculating the RMSD between experimental and redocked poses (Fig. 4). Docked conformations and protein–ligand interaction patterns were analyzed and visualized using PyMOL 2.5

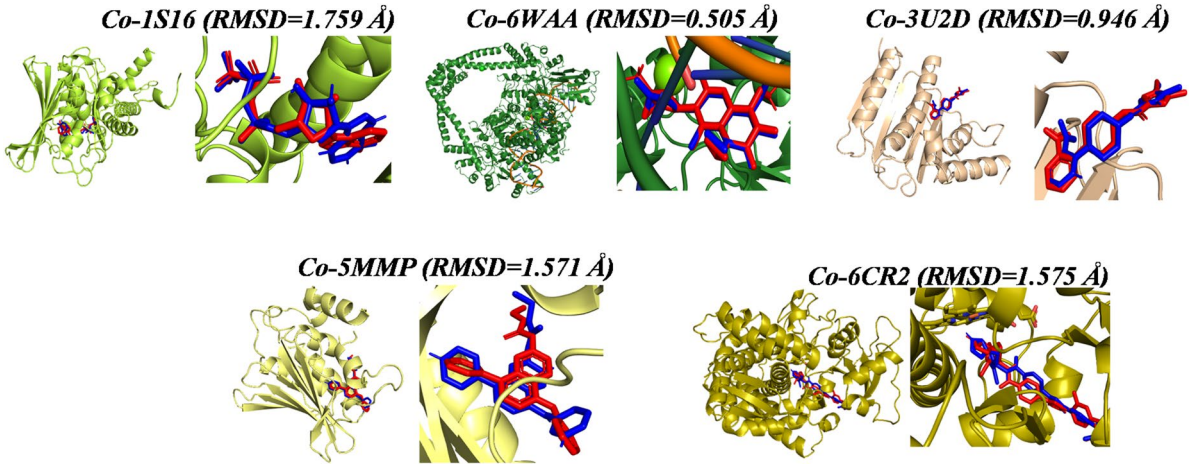

Fig. 4. Docking protocol validation by redocking of co-crystallized ligands into 1S16, 6WAA, 3U2D, 5MMP, and 6CR2, showing the superposition of native and redocked poses and the corresponding RMSD values.

Fruit	Yield							
	Color	Total weight (g)	Skin (g)	fruit (g)	length (cm)	Width (cm)	Nb Seeds per fruit	Yield (oil) (%)
OFI	Green	99.44 ± 1.54	43.67 ± 2.13	55.77 ± 1.4	6.5 ± 0.23	3.5 ± 1.01	366 ± 0.3	13.42 ± 0.12

Table 1. Morphological and physical characteristics of *Opuntia ficus indica* fruit.

Extract	Total polyphenols (mgEAG/100 g *P.S*)	Flavonoids (mg EQ/100 g *P.S*)
OFI OIL	26.3 ± 0.12	2.1 ± 0.07

Table 2. Total polyphenol and flavonoid contents.

and Discovery Studio 2024, and the final binding modes were selected based on the best docking score together with chemically plausible interactions within the targeted pocket.

Results and discussion

Phytochemical analysis of organic prickly pear seed oil

The following table presents an overview of the fruit's morphological and physical characteristics, including length, width, diameter, and weight, as well as skin and seed properties. These measurements are reported for various locations of the fruit to provide a comprehensive understanding of its variability. Morphological studies have demonstrated that the weight of OFI fruit (55.77 g) exceeds that of *Opuntia dilleni*. Extractions are obtained using a mechanical press at low temperature The oil yields from OFI seeds are reported in Table 1.

A total of 500 g of dried seeds (M2) yielded 67.10 g of oil (M1), corresponding to an extraction yield of highest proportion (13.42%) of oil[11].

Determination of total polyphenols and flavonoids

The determination of total polyphenols by the Folin-Ciocalteu method of OFI oil showed that all calibration curves show a strong positive linear correlation R Eq. 1. The results obtained from the polyphenols reported at the oil level of OFI seeds collected from the Eastern Morocco at the level of Table 2 shows that the level of total phenols is low 26.3 mgEAG/100 g these results are in agreement with Berrabeh et al. (2019)[22] who show the contents of seeds bark and pulp are the lowest and are in the vicinity of 1.38 mg/g EAG only, other studies shows a similar results that the total phenolic and flavonoid contents of *Cakile maritima* with(32.23 ± 1.97 mg GAE/g)[23].

Identification and quantification of fatty acids by GC-MS

In this study, an analysis was conducted to compare the chemical composition of organic oil from *Opuntia ficus indica* harvested in the eastern region of Morocco. The results of this analysis, including the compositions of OFI organic oil and their chromatograms, are presented in Table 3. Preliminary examination by GC-MS confirmed the presence of several fatty acids in the extract. The percentage of this fatty acid depend on the geographical and the origin of the specific fruit part. Linoleic acid represents the major fatty acid, accounting for 73.94%, while palmitic acid and stearic acid, which had moderate values of 21.08% and 4.9%, respectively.

	Opuntia ficus indica		
Fatty Acids	RT (Min)	% Air Extraction	IM
Palmitic acid, C16 :0	23.29	21.08%±0.02	MS
Linoleic acid, C18 :2	24.99	73.94%±0.04	MS
Oleic acid, C18 :1	25.03	Nd	
Stearic acid, C18 :0	24.62	4.96 ± 0.1	MS
Arachidic acid, C20 :0	25.24		MS
Fatty Acids	SFA[a]	26.04	-
	UFA[b]	73.94	-
	UFA/SFA[c]	2.83	-

Table 3. Chemical composition of *Opuntia ficus indica* seed oil. SFA: Saturated Fatty Acids UFA: Unsaturated Fatty Acids.

Notably, oleic acid was no longer detected in our OFI organic oil. The linoleic acid content of *Opuntia ficus-indica* oil exceeds that of most commonly consumed oils, including those derived from corn, soy, cottonseed and *Glacium flavum* with linoleic acid (20.00%), and alpha-linolenic acid (41.43%)[24]. fatty acid profile is relatively similar to that of safflower oil. Linoleic acid has been demonstrated to possess cholesterol-lowering properties. Stearic acid has been demonstrated to have a neutral effect on the concentration of LDL cholesterol in blood serum and has been determined to be non-toxic to human health[19]. The high level of unsaturation (particularly linoleic acid), combined with a low level of linolenic acid (C 18:3), which adversely affects oil stability, indicates that *Opuntia ficus-indica* seeds could be an excellent potential source of edible oil for human consumption. The negligible variances in oleic, linoleic, and palmitic concentrations are presumably contingent on the fruit's degree of ripeness, as well as geographical and temporal factors[20] Linoleic acid has been demonstrated to possess advantageous properties for the skin, it is utilized in the fabrication of cosmetics and pharmaceutical products. Stearic acid has been demonstrated as neutral effect with regard to LDL cholesterol regulation in blood serum and considered safe for human consumption. The unsaturation ratio (AGI/AGS) indicates a higher concentration of unsaturated fatty acids (AGI) in the fruit peel and seed (OFI) under study. These fatty acids are distinguished by their high percentage of polyunsaturated fatty acids (61 – 58%), a property that has garnered them significant recognition in the fields of nutrition and pharmaceuticals[25]. As reported Ramadan M.F. and Mörsel J.T., 2003[22], polyunsaturated fatty acids (PUFAs) are known to have a positive effect on several health conditions, including cardiovascular disorders, inflammatory, heart disease, atherosclerosis, autoimmune diseases, and diabetes. Moreover, the presence of these fatty acids in breast milk has been linked with enhanced performance in breast-fed infants compared to those on formula. The chemical composition of prickly pear oil is analogous to that of other oils frequently used in cosmetics, such as evening primrose and sunflower oil, where linoleic acid is the predominant fatty acid. These oils are frequently utilized in homeopathic remedies for dry, irritated skin as well as in cosmetics. The analysis of these values indicated that seed oils are abundant in unsaturated fatty acids, thereby substantiating their significance as a nutritional source for human consumption. These results are consistent with the findings of studies conducted by Ghazi et al. (2015), which reported linoleic acid as the predominant fatty acid, with levels reaching up to 79.83%[26]. The role of fruit ripeness is also a salient factor, given that discrepancies in the fatty acid profile and their concentrations, as reported in the extant literature, may be attributable to the methodologies employed for extraction, storage, and characterization. These methodologies, in turn, are likely influenced by genetic and social factors. As demonstrated by Coskuner et *al.*, the content of saturated fatty acids increases with the progression of ripening[23].

Identification of bio-oil volatile compounds by headspeace GC/MS The main volatile

As indicated in Table 4, the compound identified in cactus seed oil was nonanal, with an average quantity of 11.46%. As indicated by the data in Fig. 5, the aldehydes responsible for the citrus aromatic profile included decanal, (8Z)−14-methyl-8-hexadecenal, and E-11-hexadecenal. These compounds were found in *Opuntia ficus indica* oil, with different proportions (8.71%, 8.51%, and 8.33%, respectively) (Fig. 5).

Menthone was also found to be present in prickly pear seed oil, accounting for 5.39% of the oil's composition. Isopropyl Palmitate is present with a significant percentage of 3.38%, an ester of palmitic acid and isopropyl alcohol. Palmitic acid is a naturally occurring substance found in both plants and animals. This substance forms a water-resistant film on the surface of skin or hair, thereby preventing moisture from escaping. This process contributes to the preservation of skin moisture. This characteristic renders it particularly beneficial for individuals suffering from dry skin. Furthermore, the presence of a longer chain in its structure is known to enhance its affinity for the skin. Its primary function is to facilitate the movement of dry ingredients by acting as a lubricant. This process also results in a soft and smooth appearance of the skin. According to the extant literature, six volatile compounds have been identified in Italian fruits of *O. ficus-indica* 24 and 61 in Mexican fruits of *O. ficus-indica*[24], representing successively 100% and 95% of all volatile compounds in the fruits 25. Arena et al. identified six volatile compounds by GC-MS, with E-2-hexen-1-ol and hexan-1-ol as the main products, accounting for approximately 80% of the total weight of the extracts obtained by SPME. As indicated in the SMPE report, the following compounds were extracted: (E)−2-hexenal, (Z)−2-penten-1-ol, (Z)−3-hexen-1-ol, (E)−2-hexen-1-ol, (E)−2-nonen-1-ol, and (E, Z)−2,6-nonadien – 1-ol. Hexanal is a significant reaction product

	Volatile compound	RT (Min)	N° CAS	Area (%)
1	**Heptanal**	**4.825**	**111-71-7**	**3.87**
2	5-Isopropyl-2-methylbicyclo [3.1.0] hexan-2-ol	5.232	546-79-2	0.26
3	Hept-2-enal	5.751	18829-55-5	1.80
4	Heptanol	5.954	111-70-6	1.93
5	1,6-Octadien-3-ol, 3,7-dimethyl-, acétate	6.135	115-95-7	1.04
6	Octanal	6.412	124-13-0	2.46
7	Benzene, 1-ethyl-3,5-dimethyl-	6.755	934-74-7	2.81
8	1,2-Diisopropenylcyclobutane	6.947	19465-02- 2	4.57
9	(E)−2-Octen-1-al	7.314	2548-87-0	4.86
10	1-Octanol	7.565	111-87-5	2.58
11	2-Propyltetrahydro-2 H-pyran-3-yl acétate	7.861	N.D	1.72
12	Nonanal/2-Tridecen-1-ol, (E)-	8.072	124-19-6	**11.46**
13	7-Octen-3-ol, 2,3,6-trimethyl-/3-Pentanol, 2,2,4,4-tetramethyl-	8.478	118989-21-2	0.38
14	2-Nonenal, (E)-	8.969	18829-56-6	2.51
15	Menthone	9.108	89-80-5	5.39
16	9-Oxa-bicyclo[3.3.1]nonane-1,4-diol	9.459	35377-88-9	3.29
17	Hexadecanal	9.655	629-80-1	1.13
18	4-Ethylcyclohexanol/9-Oxabicyclo[3.3.1]nonan-2-ol	9.841	4534-74-1	0.52
19	2-Dodecyl-1,3-propanediol	9.974	10395-09-2	1.00
20	2-Decenal, (Z)-	10.315	2497-25-8	**8.71**
21	(8Z)−14-Methyl-8-hexadecenal	10.565	60609-53-2	**8.51**
22	Nonanoic acid, 1-methylethyl ester	10.840	28267-32-5	1.87
23	6-Methyl-bicyclo[4.2.0]octan-7-ol	11.046	N.D.	1.31
24	2,4-Dodecadienal, (E, E)-	11.187	21662-16-8	2.32
25	Undecanal/2,4-Decadienal	11.396	112-44-7	2.47
26	2-Undecenal	11.818	2463-77-6	0.95
27	Hexanal	12.063	66-25-1	**8.33**
28	2-Ethylnon-1-en-3-ol	12.138	N.D	0.89
29	2-Methyl-7-oxabicyclo [2.2.1]heptane	12.294	16325-23-8	0.64
30	Z-2-Octadecen-1-ol	12.630	2831-86-9	0.45
31	Hexadecen-1-ol, trans-9-/1-Pentadecanol	13.221	629-76-5	0.57
32	(2Z)−2-Octadecenyl acetate	13.449	N.D	0.60
33	9-Octadecen-1-ol,	14.001	143-28-2	0.40
34	Cyclododecanone, 2-methyl-	14.561	16837-94-8	0.72
35	2-Octadecyl-propane-1,3-diol	15.298	5337-61-1	0.38
36	6,6-Dimethyl-cyclohex-2-en-1-ol	15.744	38313-10-9	0.52
37	E-2-Tetradecen-1-ol	15.976	75039-86-0	0.58
38	E-15-Heptadecenal	16.033	700381-35-7	0.40
39	E, E,Z-1,3,12-Nonadecatriene-5,14-diol	16.318	N.D	0.59
40	Cycloheptadecanol	16.528	4429-77-0	0.32
41	13-Tetradecenal	17.471	85896-31-7	0.49
42	Z, Z-6,28-Heptatriactontadien-2-one	18.381	133530-21-9	0.34
43	(4Z,16Z)−4,16-Octadecadienyl acetate	18.579	60534-16-9	0.68
44	Isopropyl Palmitate	19.350	142-91-6	3.38

Table 4. Identification of volatile organic oil compounds by headspeace GC/MS. ND: None detected.

that is a byproduct of the oxidation of oleic, linoleic, and linolenic acids. It can be formed during oil processing and cleaning when the oil comes into contact with air[4].

Tocopherol content of organic OFI oil by HPLC-DAD

The determination of tocopherol values in cactus seed oils was performed using liquid chromatography (HPLC), as illustrated in Table 5. An analysis of the tocopherol content in prickly pear seed oil from our region revealed the presence of γ-tocopherols, the primary compound, with a concentration of 657.52 mg/kg, followed by α-tocopherols, ϐ-tocopherols, and β-tocopherols with concentrations of 23.02 mg/kg, 12.37 mg/kg, and 1.26 mg/kg, respectively.

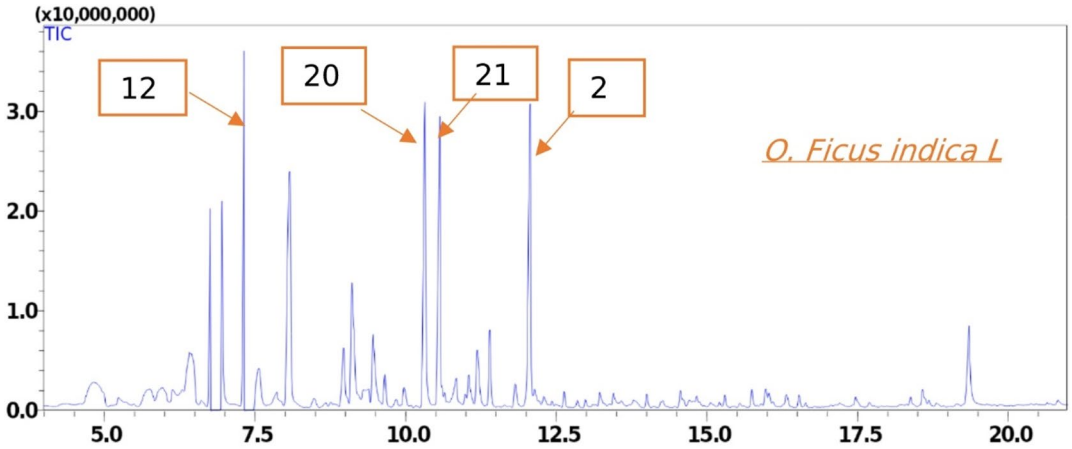

Fig. 5. volatile compounds of OFI seed oil.

	Tocopherols	Bio oil mg/kg
1	**α-tocopherols**	**23,02± 0,18**
2	β-tocopherols	1,26± 0,01
3	γ-tocopherols	657,52± 1,01
4	δ-tocopherols	12,37± 0,05
5	Total Tocopherols	694,17± 2,26

Table 5. Tocopherol content of OFI organic oil.

In the extant literature on EL, Mannoubi et al. (2009) found that γ-tocopherols appear to be the primary component of the seed oil, accounting for 94.12% of the total vitamin E content, while δ-tocopherol accounted for 3.42% of the total[2810]. The unsaponifiable portion of plant foods contains significant amounts of tocopherols. Seed oils constitute an important natural source of Vitamin E in addition to providing essential fatty acids. Tocopherols are naturally occurring antioxidants that possess biological activity. Major biochemical role of tocopherols involves safe guarding of polyunsaturated fatty acids from oxidative degradation[29]. γ-Tocopherol was identified as the predominant component of blackcurrant oil (55.4 mg/kg) and rose hip oil (71.0 mg/kg)[30]. According to Matthaus and Özcan's (2006) the mean concentrations of α-tocopherol, β-tocopherol, and γ-tocotrienol[31] in turpentine oils were, respectively, 134.9 milligrams per kilogram (mg/kg), 135.6 mg/kg, and 100.0 mg/kg. It has been demonstrated that γ-tocopherol exerts a favorable influence on human nutrition and health, attributable in part to its antioxidant potential[32].

Polyphenol identification by ultra-high performance liquid chromatography MS/MS

Polyphenol identification is presented in Table 6. Peak identification was based on retention times and mass-to-charge (m/z) ratios obtained from the analyzed standards, as well as comparison with a company-generated database comprising 50 phenolic compounds. Comprehensive evaluation of the acquired mass spectra revealed the presence of 45 compounds, with Arubtin being the major compound at 6. 709% (Table 6) followed by quercetin, hesperidin, kaempeferol, luteolein, chlorogenic acid, salicylic acid, p-coumaric acid, and trans-ferulic acid with 6.391%, 5.348%, 5.774%, 4.667%, 4.948%, 4.137%, 3.988% and 3.316%.

Phenolic constituents exhibit a strong association with antioxidant potential, and several reports have shown a linear correlation between antioxidant activity and phenolic compound content. The compounds are also recognized for contributing to various health benefits[27].

In recent years, scientific articles have been abundant on cactus and, in particular, seeds have been identified as a raw material with high amounts of phenolic compounds (Fig. 6)[28].

Because the majority of phenolic compounds remain in the press cake during oil extraction, changing the phenolic composition, previously published results on the composition of phenolic compounds in fruits or seeds are of limited use.

Specifically, costly oils like cactus seed oil are thought to be vulnerable to different forms of food fraud. Phenolic compound properties found in various vegetable oil types can be used to distinguish between oils and oil blends as well as to pinpoint the oils' place of origin[29].

Antimicrobial activity

Antimicrobial activity refers to the ability of extracts to inhibit bacterial growth in culture medium.

N°	Composants	m/z	RT (min)	AIR %
1	Gallic acid	168.9	1.2	1,358
2	Quercetin	301.0	8.0	6,391
3	p coumaric acid	162.9	4.9	3,988
4	Oleochantal	303.2	19.2	2,964
5	hydroxytyrosol	153.05	2.1	0,910
6	trans-ferulic acid	193	5.5	3,316
7	Oleuropein	539	17.5	0,804
8	Hesperidin	301.3	10.8	5,348
9	trimethoxyflavone	312	19.5	2,974
10	Arbutin	271.2	2.7	6,709
11	Rosmarinc acid	359	16.6	2,730
12	Ursolic acid	455	22.0	1,317
13	Apigenin	269	15.9	2,937
14	Amentoflavone	537.1	21.3	1,993
15	Luteolin	284.9	15.7	4,667
16	Quercetin-3-O-glucosid	463.1	8.6	3,486
17	quercetin-3-O-acid glucuronic	477	8.3	3,295
18	Kaempferol-3-O-glucose	609.1	9.0	1,024
19	Quercetin-3-O. hexose deoxyhexos	609.1	9.7	0,960
20	Isorhamnetin- 3-O Rutinoside	623.1	10.3	1,141
21	Isorhamnetin-7-O- Pentose	477.1	11.0	2,256
22	luteolin 7-O-glucoside	477.1	9.2	2,282
23	kaempferol-3-O-glucuronic	461.1	8.8	Nd
24	Kaempferol-3-O-pentose	417.1	11.2	2,844
25	Kaempferol-3-O-hexose déohyhexose	593.1	11.3	0,8569
26	Tyrosol	153.4	2.2	0,620
27	protocathécoïc acid	153	1.7	0,809
28	vanillic acid	167	2.4	1,515
29	syringic acid	197	2.6	1,676
30	p-hydroxybenzoïc acid \ salicilic	137	2.3	4,137
31	Gentisic acid	153	2.5	0,732
32	caffeic acid	179	4.1	1,599
33	sinapic acid	223	6.4	1,971
34	ferulic acid	193	5.7	2,301
35	trans-cinnamic acid	147	7.3	Nd
36	chlorogenic acid	353	4.8	4,948
37	catechin\\N-epicatechin	289	14.3	Nd
38	Gallocathéchine gallate epigallocatechin	457	14.9	2,605
39	gallocathechine - epigallocathechine	305	13.3	Nd
40	gallate catechin	441	14.0	Nd
41	Procianidine	577	21.0	Nd
42	Kaempeferol	317	16.3	5,774
43	Myricetin	285	14.4	3,449
44	Rutine	609	10.6	Nd
45	narigin	579	11.9	1,293

Table 6. Identification of polyphenols by ultra-high performance liquid chromatography mass spectrometry (UHPLC-MS/MS). Nd: Not detected.

Reported by S. Cosentino et al. (1999) and Gulfraz et al. (2008), the antibacterial activity of biological oils is largely linked to the presence of terpenoids and phenolic compounds[30]. Tiwari et al. (2009) explained that the antibacterial action of phenolic molecules is influenced by the pattern of alkyl substitution in the phenol nucleus.

After dissolving the oil and cake extracts in DMSO to create a stock solution, we diluted it several times to get half-concentrations. The antibacterial activity of the isolated molecules was evaluated using the agar diffusion method (antibiogram). Four Gram-positive and Gram-negative bacterial strains (*E. coli*, *Staphylococcus aureus*, *Streptococcus spp*, *Klebsiella spp*) were studied. The results of these tests are summarized in Table 7.

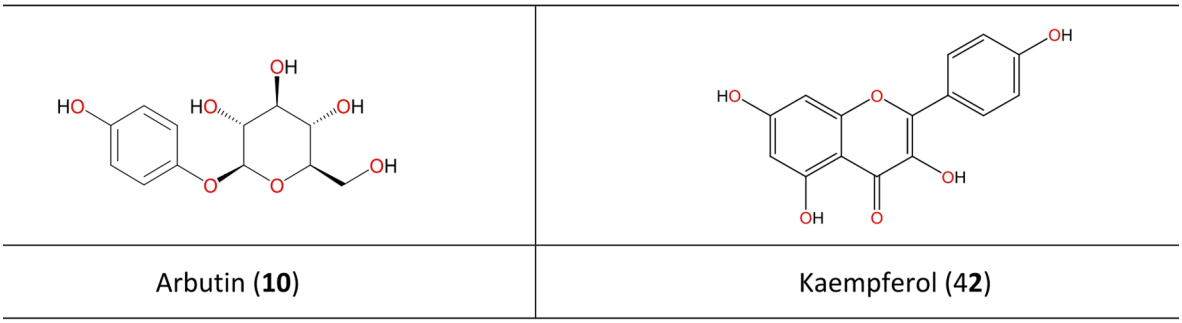

Fig. 6. Chemical structure of the two major compounds: Arbutin (**10**) and Kaempferol (42).

Extract/antibiotic	S. Aureus	Streptococcus spp	E. coli	Klebsiella spp
Inhibition zone (mm)				
OFI seed oil	NI	NI	11,6 ± 0,64	15,6 ± 0,51
C+ (Gentamicin)	41 ± 0,35	43 ± 0,38	32 ± 0,38	42 ± 1,02
Lactic acid	17 ± 0,70	21 ± 0,76	15 ± 0,64	17 ± 0,25

Table 7. Diameters (mm) of bacterial growth inhibition zones caused by methanolic extracts of oil from OFI seeds. NI: no inhibition observed (inhibition zone < 7 mm). • Diameters less than 7 mm: no antimicrobial activity. • Diameters of 7 to 9.9 mm: low antimicrobial activity. • Diameters of 10 to 11.9 mm: moderate antimicrobial activity. • Diameters of 12 to 15 mm: high antimicrobial activity d the wells.

The antibacterial results indicate that the OFI oil extract is inactive against *Staphylococcus aureus* and *Streptococcus spp*. In contrast, the oil extract shows moderate activity against the two Gram-negative bacterial strains (*Escherichia coli* and *Klebsiella spp*.), with an inhibition zone ranging from 11 to 16 mm. Vigorous antibacterial activity was observed against *Klebsiella spp*., with a zone diameter of 15.6 mm. However, the oil cake has significant antibacterial inhibitory activity against Gram-positive *Staphylococcus aureus* and *Streptococcus spp*. In general, the best results are obtained against *Streptococcus spp.*, which has an inhibition zone of 23.66 mm, followed by *Staphylococcus aureus* with an inhibition zone of 18.33 mm, compared with other plant studies like *Stachys maritima* demonstrated antimicrobial activity against *E. coli* ATCC 25,922 and *S. aureus* ATCC 25,923, with effective MIC values of 25 mg/mL and 6.25 mg/mL, respectively[32].

On the other hand, *Klebsiella spp* and *E. coli* strains show modest to low activity against these strains when exposed to oilseed meal extracts. This antibacterial activity is probably due to the presence of phenolic compounds. S. Cowan et al. demonstrate a positive correlation between phenolic compound content and antibacterial, antifungal, and antimicrobial activity (*Kumaar et al. 2013*). Polyphenols and flavonoids are critical antimicrobial substances. The primary compounds in these active extracts are arbutin and kaempferol, which possess antimicrobial properties and antioxidant capabilities. Indeed, many researchers have found that the strains' lack of sensitivity may be attributed to the method used to evaluate antimicrobial activity, which can influence the results[33].

Arbutin, a hydroquinone β-D-glucopyranoside, has recently garnered attention for its significant antibacterial properties, in addition to its well-established antioxidant and depigmenting effects. Several studies have demonstrated that arbutin and its derivatives exhibit broad-spectrum inhibitory effects against both Gram-positive and Gram-negative bacteria. According to[34], α-arbutin and β-arbutin showed stronger inhibition zones against *Escherichia coli* and *Pseudomonas aeruginosa t*han hydroquinone, indicating that the glycosidic linkage enhances the biological activity by improving molecular stability and solubility.

Furthermore, in vitro and in silico analyses by Maslov et al. (2024) confirmed the synergistic interaction of arbutin with several antibiotic classes (β-lactams, fluoroquinolones, and macrolides), suggesting that the compound may potentiate antibiotic efficacy by disrupting bacterial membrane integrity and quorum-sensing mechanisms. This synergistic behavior highlights the potential of arbutin as a natural adjuvant in antimicrobial formulations.

Additionally, arbutin-rich plant extracts, particularly those from Arctostaphylos uva-ursi and Vaccinium vitis-idaea, have been used for a long time in the treatment of urinary tract infections (UTIs) due to their antiseptic and bacteriostatic properties[35]. Recent pharmacological reviews have confirmed that the hydroquinone moiety of arbutin is gradually released via enzymatic hydrolysis, generating active intermediates that contribute to inhibiting microbial growth. Kaempferol, a naturally occurring flavonol widely distributed in fruits, vegetables, and medicinal plants such as *Opuntia ficus-indica*, Camellia sinensis, and Ginkgo biloba, has been reported to exhibit broad-spectrum antibacterial activity. Its molecular structure, characterized by four hydroxyl groups (3, 5, 7, and 4′), plays a crucial role in binding to bacterial cell wall proteins and disrupting membrane permeability, leading to cell lysis and growth inhibition[36].

Several studies have demonstrated that kaempferol and its glycosides exhibit notable inhibitory effects against both Gram-positive and Gram-negative bacteria, including *S. aureus*, *Bacillus subtilis*, *E. coli*, and *Pseudomonas aeruginosa*[37]. The compound acts through multiple mechanisms, including the inhibition of DNA gyrase and topoisomerase IV, disruption of bacterial biofilm formation, and chelation of metal ions required for enzymatic activity.

Several studies have highlighted the high sensitivity of Gram (+) bacteria compared to Gram (-) bacteria[38], which can be attributed to the difference in the outer layers of Gram (-) and Gram (+) bacteria. The antimicrobial activity of oils is generally more effective against Gram-positive than against Gram-negative bacteria, which are more resistant mainly because their outer membranes are less permeable[40]. The biological activity of an essential oil is linked to its chemical composition, the functional groups of the major compounds (alcohols, phenols, terpenic and ketonic compounds), and their synergistic effects. Several studies have demonstrated the occurrence of potassium ion leakage in the microbial cells of *E. coli* and *S. aureus* upon exposure to oil[41]. This potassium leakage is the first evidence of irreversible damage to the bacterial membrane. Some of the active components of essential oils make the bacterial membrane permeable, a precursor to bacterial death. *Opuntia ficus-indica* oil has many bacteriostatic properties. Differences in antimicrobial activity levels may be related to the chemical composition of the oils. Mnayer et al. (2014) suggest that the compounds in the oil may act on different bacterial strains[42]. Furthermore, the selectivity of oils towards certain bacteria remains poorly understood. This selectivity results from the varied composition of the active fractions in the oils, which often exhibit synergistic actions[43].

Antifungal activity

Antifungal activity against Fusarium *Oxysporum Albidinis*. The entire experiment was repeated three times, and relative growth in the presence of the extract was measured in relation to that of cultured yeast. Methanolic extracts of oils are inactive against all strains tested.

POM Analysis of the two major compounds of *Opuntia ficus-indica (L) Mill*

POM Theory simplifies the determination of the pharmacophore site(s) for each compound and enables precise forecasting of its antiviral, antifungal, antibacterial, and antitumor properties (Fig. 7). It is a constitution of three programs:

- https://docs.chemaxon.com/display/lts-europium/marvinsketch-downloads.
- https://www.organic-chemistry.org/prog/peo/.
- https://www.molinspiration.com/.

The Osiris and Molinspiration prediction of Toxicity, Drug-score of **10** and **42** (Table 8**)** show that compounds present limited side effects and encouraging Drug score of 38% and 46% respectively for compounds **10** and **42.** On other hand, both compounds meet Lipinski 5 rules; there is no violation (NV = 0). The atomic charge calculations of compounds **10** and **42** indicate that the two compounds are bearing antibacterial ($OH^{\delta+}$----$O^{\delta-}$) pharmacophore sites (Fig. 7; Table 8).

If the identification of the antibacterial ($OH^{\delta+}$----$O^{\delta-}$) pharmacophore site of compound **42** is evident and easy, because of its partially rigid structure, the compound **10** needs more efforts because of its large number of rotatable bonds (Fig. 8).

Figure 8 has been of great help to identify the antibacterial ($OH^{\delta+}$---$O^{\delta-}$) pharmacophore site of each compound **10** and **42** with high precision. **Recently**, Maslov et al., 2024a and 2024b confirmed experimentally the antibacterial of compound **10**[34]. So our virtual POM calculations converge perfectly with those experimental results.

Molecular docking

Molecular docking was employed as a structure-based complement to our POM-based chemical profiling and antimicrobial assays, allowing us to move beyond compound identification toward a mechanistic interpretation by predicting the most probable binding poses, key stabilizing interactions, and relative binding tendencies of the major constituents arbutin (10) and kaempferol (42) within biologically relevant targets[51,52–53].

Because the extracts exhibited antibacterial effects across both Gram-positive (*Staphylococcus*/*Streptococcus*) and Gram-negative (*E. coli*/*Klebsiella*) strains, we prioritized type II bacterial topoisomerases essential enzymes that govern DNA replication and chromosome segregation and that represent well-established antibacterial drug targets. Accordingly, we selected high-quality crystallographic models with well-defined active sites and co-crystallized ligands that reliably delineate the functional binding pockets: 3U2D (*S. aureus* GyrB ATPase domain) and 5MMP (*E. coli* GyrB) to represent the conserved gyrase ATPase pocket in Gram-positive and Gram-negative bacteria, together with 1S16 (*E. coli* ParE ATPase domain) and 6WAA (Topoisomerase IV ParE–ParC in a DNA-associated complex) to capture the complementary topoisomerase IV sites frequently implicated in antibacterial activity[54]. Finally, to help rationalize the lack of antifungal activity observed against Fusarium, we included 6CR2 (fungal CYP51B)[55], a canonical azole-responsive sterol biosynthesis target, to assess whether compounds 10 and 42 are structurally compatible with the sterol 14α-demethylase active site[56].

Table 9 indicates that, among the two investigated metabolites, kaempferol (42) consistently exhibits the most favorable predicted binding across the selected targets, with its two best docking scores obtained for the *E. coli* topoisomerase IV ParE ATPase domain (1S16, −8.9 kcal/mol) and the fungal sterol 14α-demethylase CYP51B (6CR2, −8.7 kcal/mol), whereas arbutin (10) shows moderate but still meaningful affinities (e.g., −7.4 kcal/mol on 1S16 and − 7.6 kcal/mol on 6CR2)[57,58]. In contrast, both ligands display weak binding in the 6WAA model (−3.7 to −3.9 kcal/mol), close to the co-crystallized reference (−4.0 kcal/mol), suggesting that within topoisomerase

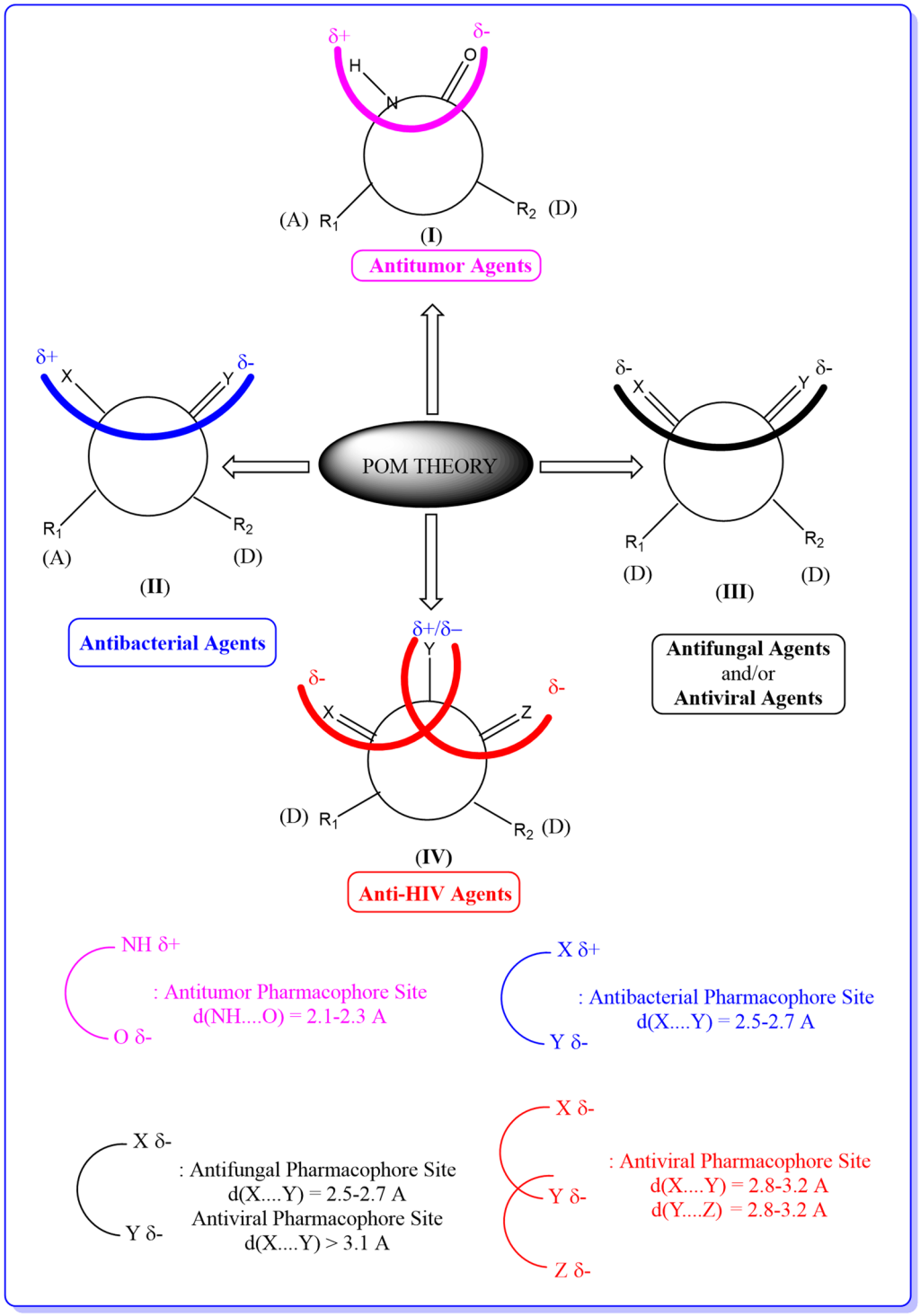

Fig. 7. Organigram of POM Theory showing the structure of principal pharmacophore sites, as antibacterial[44,45], antifungal[46], antiviral[47,48], and antitumor[49] drugs.

IV the ATPase pocket is a more plausible binding region for these phenolics than the DNA-cleavage/quinolone-associated site represented by 6WAA. In the bacterial gyrase models, kaempferol also shows favorable energies (3U2D, −7.7; 5MMP, −7.1 kcal/mol), and notably its score in 3U2D is very close to the co-crystallized ligand (−7.6 kcal/mol), supporting a credible accommodation within the GyrB ATPase pocket and providing a mechanistic rationale for the antibacterial activity observed experimentally[59]. The interaction analysis of the two best-scoring complexes (Fig. 9) reinforces this interpretation: in 1S16, kaempferol is stabilized by a conventional hydrogen bond with Asp1069, complemented by a π–anion interaction with Glu1046 and hydrophobic π-alkyl contacts with Met1074 and Ile1090 (with an additional carbon-hydrogen interaction involving Pro1075), which

Toxicity and Drug-score prediction	Lipinski 5 rules	Atomic charge	3D presentation Antibacterial site
 Compound **10**	miLogP -0.81 TPSA 119.61 MW 272.25 nON 7 nOHNH 5 nviolations 0 volume 232.20	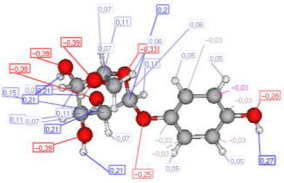	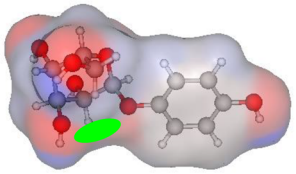
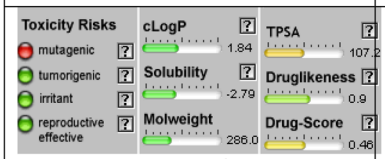 Compound **42**	miLogP 2.17 TPSA 111.12 MW 286.24 nON 6 nOHNH 4 nviolations 0 volume 232.07	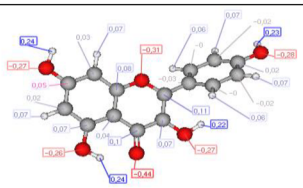	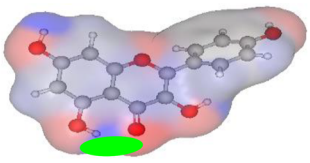

Table 8. Osiris, Molinspiration, atomic charge, and prediction of Toxicity, Drug-score of **10** and **42.**

Co mpd	2D Structure	3D Structure	potential antibacterial ($OH^{\delta+}$---$O^{\delta-}$) pharmacophore site [50]
10	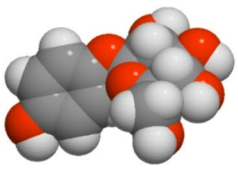	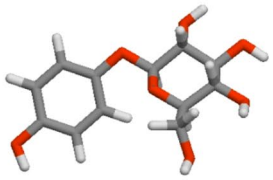	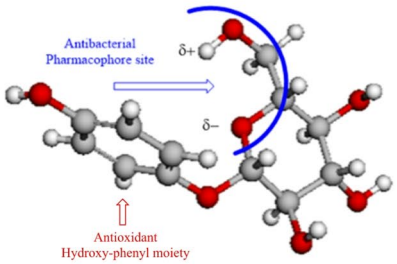
42	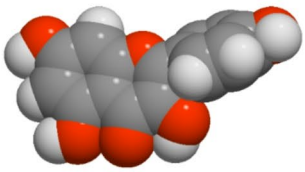	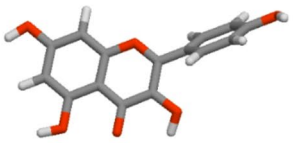	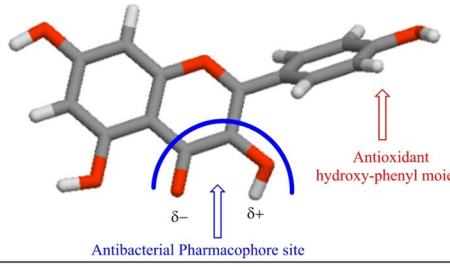

Fig. 8. 3D structural optimization and identification of antibacterial pharmacophore sites of compounds **10** and **42**.

together favor tight packing in the nucleotide-binding site; in 6CR2, kaempferol is mainly retained through aromatic/hydrophobic contacts, including a π–π T-shaped interaction with Tyr122 and π-alkyl contacts with Ala307 and Leu503, indicating that the CYP51B cavity can accommodate the ligand but that stabilization is dominated by nonpolar interactions an observation that can help rationalize why a good docking score may not necessarily translate into antifungal efficacy in vitro, where target engagement requirements and cellular access can be decisive[60].

Conclusion

For the first time, the current study provides a comprehensive characterization of *Opuntia ficus-indica* seed oil and its residues, revealing their remarkable biochemical richness and biotechnological potential. The results demonstrated that these matrices represent an excellent natural source of tocopherols, polyphenols, and essential fatty acids, predominantly of linoleic acids, which are known to play key roles in maintaining oxidative stability and promoting biological activity. The high levels of γ-tocopherol and phenolic compounds underscore the oil's strong antioxidant potential. At the same time, the presence of bioactive flavonoids, such as kaempferol and arbutin, suggests additional pharmacological properties, including anti-inflammatory and antibacterial effects.

Binding Energy (Kcal/mol)					
PDB code/compounds	**1S16**	**6WAA**	**3U2D**	**5MMP**	**6CR2**
Arbutin	−7.4	−3.7	−7.1	−6.3	−7.6
Kaempferol	−8.9	−3.9	−7.7	−7.1	−8.7
Co-1S16	−11.5	N/A	N/A	N/A	N/A
Co-6WAA	N/A	−4.0	N/A	N/A	N/A
Co-3U2D	N/A	N/A	−7.6	N/A	N/A
Co-5MMP	N/A	N/A	N/A	−9.3	N/A
Co-6CR2	N/A	N/A	N/A	N/A	−9.1

Table 9. Predicted binding energies (kcal/mol) of arbutin (**10**) and kaempferol (**42**) against selected bacterial topoisomerase targets (GyrB and topoisomerase IV) and fungal CYP51B, compared with co-crystallized reference ligands.

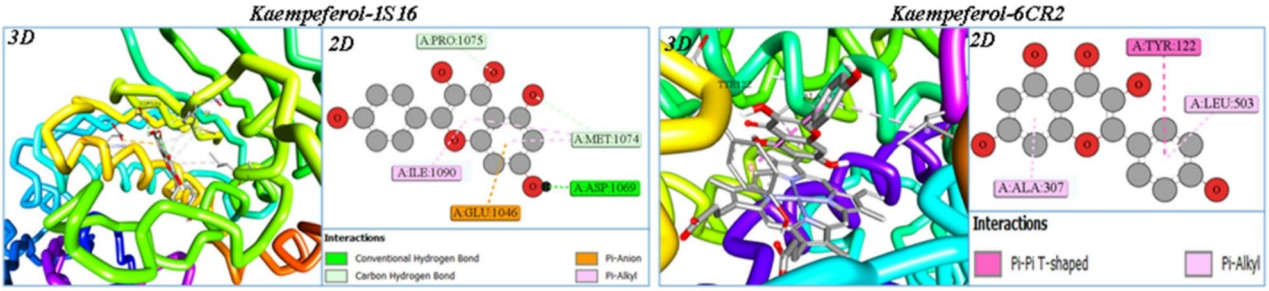

Fig. 9. 3D binding poses and 2D interaction maps of kaempferol (42) in the *E. coli* topoisomerase IV ParE ATPase domain (PDB: 1S16) and fungal CYP51B (PDB: 6CR2).

These findings collectively suggest that *O. ficus-indica* oil has a multifunctional nature, making it a valuable bioactive ingredient for various industrial applications. Overall, the valorization of these by-products offers a sustainable opportunity to convert agricultural residues into high-value materials for the food, cosmetic, and pharmaceutical sectors. Further studies integrating in vivo assays, formulation testing, and molecular modeling are recommended to deepen our understanding of their mechanisms of action and to support the development of novel natural-based products derived from this underexploited plant resource. POM Theory calculations have been beneficial in identifying compounds with attractive pharmaceutical profiles.

Data availability

The datasets used and/or analyzed during the current study are available from the corresponding author on reasonable request.

Received: 13 October 2025; Accepted: 20 February 2026
Published online: 27 February 2026

References

1. Nounah, I. et al. Effect of seed's geographical origin on cactus oil physico-chemical characteristics, oxidative stability, and antioxidant activity. *Food Chemistry: X* **22**, 101445 (2024).
2. Chekkal, F. et al. Deep learning for chemical classification and valorization of *Opuntia ficus-indica* by-products. *S. Afr. J. Bot.* **178**, 411–423 (2025).
3. Chbani, M. et al. Characterization of phenolic compounds extracted from cold pressed cactus (*Opuntia ficus-indica* L.) seed oil and the effect of roasting on their composition. *Foods* **9**, 1098 (2020).
4. Nounah, I. et al. Profile of volatile aroma-active compounds of cactus seed oil (*Opuntia ficus-indica*) from different locations in Morocco and their fate during seed roasting. *Foods* **9**, 1280 (2020).
5. Maliar, T. et al. The adapted POM analysis of avenanthramides in silico. *Pharmaceuticals* **16**, 717 (2023).
6. Elsayed, D. A. et al. Bio-computational modeling, POM analysis and molecular dynamic simulation for novel synthetic quinolone and benzo [d][1, 3] oxazine candidates as antimicrobial inhibitors. *Sci. Rep.* **14**, 28709 (2024).
7. Bouhrim, M. et al. Phytochemistry and biological activities of *Opuntia* seed oils: *Opuntia dillenii* (Ker Gawl.) Haw. and *Opuntia ficus-indica* (L.) Mill. A review. *Herba Pol.* **67**, 49–64 (2021).
8. Kadda, S., Belabed, A., Loukili, E. H., Hammouti, B. & Fadlaoui, S. Temperature and extraction methods effects on yields, fatty acids, and tocopherols of prickly pear (Opuntia ficus-indica L.) seed oil of eastern region of Morocco. *Environ. Sci. Pollut. Res. Int.* **29**(1), 158–166 (2022).
9. Abdelwahab, R. *Effet du stress salin sur les bactéries du sol: rôle d'extraits dérivés de Enteromorpha intestinalis, Ulva lactuca et Opuntia ficus-indica sur la relation bactérie-plante sous stress salin* (Université Ferhat Abbas Sétif, 2017).
10. Habibi, Y. *Contribution à l'étude morphologique, ultrastructurale et chimique de la figue de barbarie. Les polysaccharides pariétaux: charactérisation et modification chimique* (Université Joseph-Fourier-Grenoble I, 2004).

11. Kadda, S. et al. Phytochemical analysis for the residues of *Opuntia ficus indica* l seed oil of eastern region of Morocco. *Mater. Today Proc.* **72**, 3662–3668 (2023).
12. Loukili, E. H. et al. Chemical composition, antibacterial, antifungal and antidiabetic activities of ethanolic extracts of *Opuntia dillenii* fruits collected from Morocco. *J. Food Qual.* **2022**, 9471239 (2022).
13. Micalizzi, G., Dugo, P. & Mondello, L. Evaluation of Fatty Acids Profiling in a Blood Drop Spotted on DBS Card by using a Robot-assisted GC Method. (2021).
14. Loukili, E. H. et al. Inhibition of carbohydrate digestive enzymes by a complementary essential oil blend: In silico and mixture design approaches. *Front. Pharmacol.* **16**, 1522124 (2025).
15. Mikaia, A. et al. NIST standard reference database 1A. *Standard Reference Data* (2014).
16. Wang, X., Zhao, Y., Sun, P., Ji, M. & Bao, M. Automatic integration method for single and multiple peaks in the GC and GC-MS chromatograms of characteristic oil compounds. *Anal. Methods.* **7**, 2670–2679 (2015).
17. Draoui, Y. et al. Novel family of bis-pyrazole coordination complexes as potent antibacterial and antifungal agents. *RSC Adv.* **12**, 17755–17764 (2022).
18. Ponce, A., Fritz, R., Del Valle, C. & Roura, S. Antimicrobial activity of essential oils on the native microflora of organic Swiss chard. *LWT Food Sci. Technol.* **36**, 679–684 (2003).
19. Bahjou, Y. et al. High inhibition for a CoII tetrazole bi-pyrazole dinuclear complex against Fusarium Oxysporum f. sp. Albedinis. *Eur. J. Inorg. Chem.* **27**, e202300634 (2024).
20. Eberhardt, J., Santos-Martins, D., Tillack, A. F. & Forli, S. AutoDock Vina 1. 2. 0: New docking methods, expanded force field, and python bindings. *J. Chem. Inf. Model.* **61**, 3891–3898 (2021).
21. Varga, M. et al. Giving an enzyme scissors: Serotonin derivatives as potent organocatalytic switches for DNA repair enzyme OGG1. *J. Med. Chem.* **68**, 22455–22483 (2025).
22. Berrabah, H., Taïbi, K., Ait Abderrahim, L. & Boussaid, M. Phytochemical composition and antioxidant properties of prickly pear (*Opuntia ficus-indica* L.) flowers from the Algerian germplasm. *J. Food Meas. Charact.* **13**, 1166–1174 (2019).
23. Aytar, E. C. et al. Molecular docking analyses on the chemical profile and antioxidant potential of *Cakile maritima* using GC–MS and HPLC. *Sci. Rep.* **15**, 1–22 (2025).
24. Aytar, E. C. *Glacium flavum*-derived phytochemical compounds and their molecular Interactions with SIRT1. *ChemistrySelect* **9**, e202403811 (2024).
25. Chougui, N. et al. Oil composition and characterisation of phenolic compounds of *Opuntia ficus-indica* seeds. *Food Chem.* **139**, 796–803 (2013).
26. Ghazi, Z. et al. Corrosion inhibition by naturally occurring substance containing Opuntia-Ficus Indica extract on the corrosion of steel in hydrochloric acid. *J. Chem. Pharm. Res.* **6**, 1417–1425 (2014).
27. Visioli, F., Borsani, L. & Galli, C. Diet and prevention of coronary heart disease: The potential role of phytochemicals. *Cardiovasc. Res.* **47**, 419–425 (2000).
28. OUMATOU, J. et al. Volatile constituents and polyphenol composition of Opuntia ficus-indica (L.) Mill from Morocco. *Revue Marocaine des Sciences Agronomiques et Vétérinaires* 4 (2016).
29. Boutakiout, A. *Etude physico-chimique, biochimique et stabilité d'un nouveau produit: jus de cladode du figuier de Barbarie marocain (Opuntia ficus-indica et Opuntia megacantha)*, Angers, (2015).
30. Cosentino, S. et al. In-vitro antimicrobial activity and chemical composition of Sardinian thymus essential oils. *Lett. Appl. Microbiol.* **29**, 130–135 (1999).
31. Gulfraz, M. et al. Composition and antimicrobial properties of essential oil of Foeniculum vulgare. *African J. Biotechnology* **7** (2008).
32. Can Aytar, E. Antioxidant and antimicrobial properties of *Stachys maritima* via quantum dots and molecular docking. *Chemistry & Biodiversity* **21**, e202401057 (2024).
33. Boyanova, L. et al. Activity of Bulgarian propolis against 94 *Helicobacter pylori* strains in vitro by agar-well diffusion, agar dilution and disc diffusion methods. *J. Med. Microbiol.* **54**, 481–483 (2005).
34. Maslov, O. et al. Antimicrobial action of α-arbutin, β-arbutin and hydroquinone: truth and fiction. *Ann. Mechnikov's Inst.* (3), 10–19 (2024).
35. Quintus, J., Kovar, K. A., Link, P. & Hamacher, H. Urinary excretion of arbutin metabolites after oral administration of bearberry leaf extracts. *Planta Med.* **71**, 147–152 (2005).
36. Xie, J.-H. et al. Advances on bioactive polysaccharides from medicinal plants. *Crit. Rev. Food Sci. Nutr.* **56**, S60–S84 (2016).
37. Cushnie, T. T. & Lamb, A. J. Recent advances in understanding the antibacterial properties of flavonoids. *Int. J. Antimicrob. Agents* **38**, 99–107 (2011).
38. Turkmen, N., Velioglu, Y. S., Sari, F. & Polat, G. Effect of extraction conditions on measured total polyphenol contents and antioxidant and antibacterial activities of black tea. *Molecules* **12**, 484–496 (2007).
39. Falleh, H. et al. Phenolic composition of *Cynara cardunculus* L. organs, and their biological activities. *C. R. Biol.* **331**, 372–379 (2008).
40. Reyes-Agüero, J. A., Aguirre-Rivera, J. R. & Hernández, H. M. Systematyc notes and a detailed description of *Opuntia ficus-indica* (L) Mill.(CACTACEAE). *Agrociencia* **39**, 395–408 (2005).
41. Spellberg, B. & Ibrahim, A. S. Recent advances in the treatment of mucormycosis. *Curr. Infect. Dis. Rep.* **12**, 423–429 (2010).
42. Mnayer, D. et al. Chemical composition, antibacterial and antioxidant activities of six essentials oils from the Alliaceae family. *Molecules* **19**, 20034–20053 (2014).
43. Hammer, K. A., Carson, C. F. & Riley, T. V. Antimicrobial activity of essential oils and other plant extracts. *J. Appl. Microbiol.* **86**, 985–990 (1999).
44. Grib, I. et al. Novel N-sulfonylphthalimides: Efficient synthesis, X-ray characterization, spectral investigations, POM analyses, DFT computations and antibacterial activity. *J. Mol. Struct.* **1217**, 128423 (2020).
45. Lakhrissi, Y. et al. Synthesis, structural confirmation, antibacterial properties and bio-informatics computational analyses of new pyrrole based on 8-hydroxyquinoline. *J. Mol. Struct.* **1259**, 132683 (2022).
46. Al-Maqtari, H. M. et al. Synthesis, characterization, POM analysis and antifungal activity of novel heterocyclic chalcone derivatives containing acylated pyrazole. *Res. Chem. Intermed.* **43**, 1893–1907 (2017).
47. Aljofan, M. et al. Anti-hepatitis B activity of isoquinoline alkaloids of plant origin. *Arch. Virol.* **159**, 1119–1128 (2014).
48. Hosen, M. A. et al. Synthesis, antimicrobial, molecular docking and molecular dynamics studies of lauroyl thymidine analogs against SARS-CoV-2: POM study and identification of the pharmacophore sites. *Bioorg. Chem.* **125**, 105850 (2022).
49. Bechlem, K. et al. Synthesis, X-ray crystallographic study and molecular docking of new α-sulfamidophosphonates: POM analyses of their cytotoxic activity. *J. Mol. Struct.* **1210**, 127990 (2020).
50. Rego, N. & Koes, D. 3Dmol. js: Molecular visualization with WebGL. *Bioinformatics* **31**, 1322–1324 (2015).
51. Kappan, M. M. & George, J. In silico pharmacokinetic and molecular docking studies of natural plants against essential protein KRAS for treatment of pancreatic cancer. *arXiv preprint arXiv:2412.06237* (2024).
52. Yenigun, S. et al. DNA protection, molecular docking, molecular dynamic, enzyme inhibition, and kinetics studies of apigenin isolated from *Nepeta baytopii* Hedge & Lamond by bioactivity-guided fractionation. *J. Biomol. Struct. Dyn.* **43**, 9404–9415 (2025).
53. Yenigun, S. et al. Chemical constituents and bioactivities of nepeta taxa essential oils from turkey: Principal component analysis, molecular docking study, molecular dynamics, mm-pbsa and drug-likeness estimation. *ChemistrySelect* **9**, e202400583 (2024).

54. Gül, F., Demirtaş, İ, Başar, Y. & Behçet, L. Effect of harvesting at different times on antioxidant potential and phytochemical contents of *Kickxia lanigera* and *Kickxia spuria* subsp. *integrifolia*: In vitro and in silico studies. *Flavour Fragr. J.* **41**(2), 333–345. https://doi.org/10.1002/ffj.70044 (2026).
55. Aytar, E. C., Aydın, B., Torunoğlu, E. I. & Durmaz, A. Antimicrobial activity and molecular docking analysis of *Salsola kali*: Investigating potent biological interactions and chemical composition. *J. Herb. Med.* **48**, 100942 (2024).
56. Zhang, J. et al. The fungal CYP51s: Their functions, structures, related drug resistance, and inhibitors. *Front. Microbiol.* **10**, 691 (2019).
57. Khibech, O. et al. CNS-safe flavone analogues as dual SARS-CoV-2 inhibitors: an integrated in-silico design study. *ChemPhysMater*. https://doi.org/10.1016/j.chphma.2025.10.007 (2025).
58. Khibech, O. et al. Elucidating the isorhamnetin-3-O-glucoside-iNOS interaction via molecular dynamics and Hirshfeld surface analyses. *PLoS One* **20**, e0339357 (2025).
59. Bouammali, H. et al. Dual COX/5-LOX Inhibition by Isorhamnetin-3-O-Glucoside from Anthyllis cytisoides: An Integrated Chemical-Enzymatic-Computational Study. *J. Ethnopharmacol.* **358**, 120982 (2026).
60. Ibok, M. G. et al. GC–MS Characterisation, In Vitro Bioactivities, In Silico Molecular Docking and ADMET Studies of Phytoconstituents From Rytigynia umbellulata (Hiern) Robyns Essential Oils. *Flavour Fragr. J.* **41**(2), 346–361 (2026).

Acknowledgements

The authors wish to thank the Euro-Mediterranean University of Fes (UEMF), the president Pr. Mostapha Bousmina and the Mohammed First University of Oujda (UMP) for funding this research under the Fundamental Research Facilities.

Author contributions

SK performed the experiments and wrote the paper. RC is responsible for table resources. El HL, SO, and BH read and correct the paper. TB and AK analyzed the data. AB and HS are responsible for resources and figures. TBH and OK executed and interpreted the bioinformatic POM analysis and compared it with experimental data. SJ and KA wrote and edit the entire manuscript. All the authors read and contributed to the submitted version of the manuscript.

Declarations

Competing interests

The authors declare no competing interests.

Additional information

Correspondence and requests for materials should be addressed to S.K. or S.J.

Reprints and permissions information is available at www.nature.com/reprints.

Publisher's note Springer Nature remains neutral with regard to jurisdictional claims in published maps and institutional affiliations.